JOURNAL OF MATERIALS SCIENCE 16 (1981) 1956–1974

Yield and transient effects during the plastic deformation of solid polymers

C. G'SELL
Laboratoire de Physique du Solide (LA au CNRS no. 155), Ensmim, Parc de Saurupt, 54042 Nancy, France

J. J. JONAS
Department of Mining and Metallurgical Engineering, McGill University, 3450 University Street, Montreal, Canada H3A 2A7

Tensile tests were performed on seven commercial polymers at 22° C and at constant true strain rates of 10^{-4} to 10^{-1} sec^{-1}. The constant strain rates were imposed on the minimum section of each sample with the aid of a diametral transducer, an exponential function generator and a closed-loop hydraulic testing machine. The polymers investigated were: high and low density polyethylene, polytetrafluoroethylene, polypropylene, polyvinylchloride and polyamide 6 and 66. True yield drops were observed in the rigid glassy polymers, whereas yielding was more gradual in the semi-crystalline or plasticized polymers. Strain rate change tests were also performed, during which one order of magnitude increases and decreases were imposed on the specimens. "Normal" transients were observed at small strains in the samples containing a rubbery phase, while the transients were of an "inverse" nature in the samples containing a glassy phase. With an increase in the strain at which the change was initiated, the "normal" transients changed in character to "inverse". Transient tests were also performed in which straining was interrupted to permit a period of stress relaxation or of holding in the unloaded condition prior to the resumption of straining. A quantitative model is proposed, based on the dynamics of plastic waves which accounts for the transition from "normal" to "inverse" transient behaviour with increasing strain, and also explains the opposite effects of stress relaxation and of specimen unloading on the restraining transients.

1. Introduction

The plastic behaviour of solid polymers is less well understood than that of most other industrial materials. This is in spite of the numerous experimental papers which have been published describing the necking and cold drawing of various compounds. Although considerable data are now available (e.g. yield stresses and natural draw ratios), and the fine microstructure of the molecular chains has also been well characterized, the intrinsic stress–strain plastic properties are difficult to separate from the more arbitrary geometric and transient effects. The latter play a particular role at yielding and after rapid strain rate changes.

In the experiments to be described below, the geometric effects were largely eliminated through the use of a servo-controlled testing procedure which maintained a constant true strain rate at a particular location in the specimen [1]. In this way, the *intrinsic* material behaviour could be determined under constant strain rate conditions. In order to provide further information concerning the mechanisms of flow, a series of "transient" experiments was performed in which: (i) the strain rate was changed abruptly, or (ii) straining was interrupted to permit a period of stress relaxation prior to the resumption of straining, or (ii) straining was interrrupted and the samples were unloaded completely from various intervals prior to the

0022–2461/81/071956–19$03.90/0

resumption of straining. The results of these tests were interpreted by distinguishing between the elastic, viscoelastic and plastic components of the strain rate and then drawing up a quantitative model for the flow behaviour based on the dynamics of plastic waves. This model is capable of explaining the transition from "normal" to "inverse" transient behaviour during the deformation of low and high density polyethylene, and also accounts for the opposite effects of stress relaxation and of specimen unloading on the transients observed after the resumption of straining in both crystalline and glassy polymers.

2. Experimental techniques and constant strain rate results

2.1. Tensile testing procedure at constant true strain rate

Most of the studies devoted hitherto to characterization of the plastic behaviour of polymers were based on data from conventional tensile tests performed at constant rates of elongation. It was shown in an earlier paper [1] that the conventional tensile test was inconvenient for materials exhibiting early necking since the engineering stress–strain curves which can be derived from it reflect only the mean evolution of the specimens (inasmuch as the deformation is inhomogeneous), rather than the intrinsic properties of the material. In that paper a new tensile technique which controls the local true strain at the neck of a cylindrical specimen $\epsilon = 2\ln(D_0/D)$ was proposed, where D_0 and D are the initial and current diameter of the neck, (the latter recorded continuously with a diametral transducer). A constant true strain rate $\dot{\epsilon}$ was imposed by means of an MTS* closed-loop hydraulic tensile machine. The exponential function generator, which provided the control voltage, made it possible to perform not only uninterrupted constant strain rate tests, but rapid strain rate change experiments as well, in addition to stress relaxation at constant total true strain, following a special procedure which will be described below. According to this method, the true stress σ is defined by the force per unit current cross-section of the neck $\sigma = 4F/\pi D^2$. This expression ignores, for simplicity, the influence of stress triaxiality within the neck, as this has been shown to affect the value of the true stress by only a few per cent [2–5].

*MTS = Materials Testing Systems.

2.2. Characteristics of the tested specimens

Since the tensile testing procedure is based on local strain data, it was more convenient to reduce the deforming length of the samples and to impose the location of the neck by using hour glass shaped round specimens. These were machined on a lathe out of 12 mm diameter extruded rods with a minimum initial diameter equal to 6 mm.

Seven commercial polymers were investigated in this work. Four of them were tested intensively: high density and low density polyethylene (from Union Carbide, DMDY and DFDY natural, densities: 0.956 and 0.921), polyvinylchloride (from Carlew Chemicals, D101 dark grey) and polypropylene (from Hercules Canada, Profax 6823). The other three were tested to provide complementary information. These were: polyamide nylon 6, polyamide nylon 66 and polytetrafluoroethylene (Teflon). The tests were all performed at room temperature ($T_R = 22 \pm 1°C$) with slow strain rates ranging from 10^{-4} to $10^{-1}\,sec^{-1}$. This range of strain rates was chosen in order to keep the temperature rise due to heat dissipation while straining as small as possible and to ensure that the actuator of the tensile machine followed the control signal without delay or overshoot effects.

2.3. Plastic behaviour of the polymers at constant true strain rate

The plastic response of the above mentioned materials is presented in Fig. 1 in the form of experimental load against diameter curves obtained at a constant true strain rate of $10^{-3}\,sec^{-1}$. It should be noted that, as for engineering stress–strain curves obtained from conventional tensile tests, most of the curves exhibited a marked load drop at yielding. On the other hand, the usual cold-drawing plateau is absent since it corresponds in the conventional test to the propagation of the neck and is not in fact associated with a marked decrease in general neck diameter. After transformation of the curves into true stress against true strain plots, the curves of Fig. 2 are obtained, which represent the intrinsic tensile behaviour of the materials at $10^{-3}\,sec^{-1}$. The curves are characterized by two distinct stages: (i) an initial pseudo-elastic stage with a high elastic modulus and (ii) a long plastic stage, whose general feature is a gradually increasing slope $d\sigma/d\epsilon$. The transition between these two stages constitutes the yielding stage, which has different features in the different

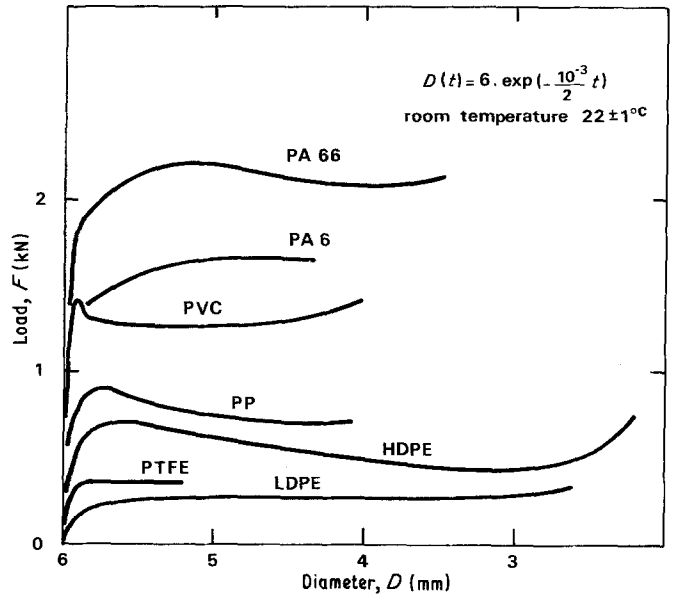

Figure 1 Experimental load against diameter curves recorded during the testing of the present seven polymers at a constant true strain rate $\dot{\epsilon} = 10^{-3}$ sec^{-1} (LDPE and HDPE: low and high density polyethylene, PTFE: polytetrafluoroethylene, PP: polypropylene, PVC: polyvinyl chloride, PA 6 and PA 66: polyamide 6 and 66).

polymers, and which will be described in more detail in the section that follows.

The influence of strain rate on the plastic behaviour after passing through the initial transient associated with yielding was determined by running a series of experiments at increasing strain rates. An example of the results obtained is illustrated in Fig. 3 for the case of HDPE. It is evident that the true stress at a given strain increases gradually with strain rate. The influence of $\dot{\epsilon}$ on σ was studied systematically in the different polymers, which revealed that this effect is not very large. (Expressed as a conventional rate sensitivity, $m = (\mathrm{d} \ln \sigma / \mathrm{d} \ln \dot{\epsilon})_{\epsilon}$, a range of 0.02 (PVC) to 0.06 (polyethylene) was observed.)

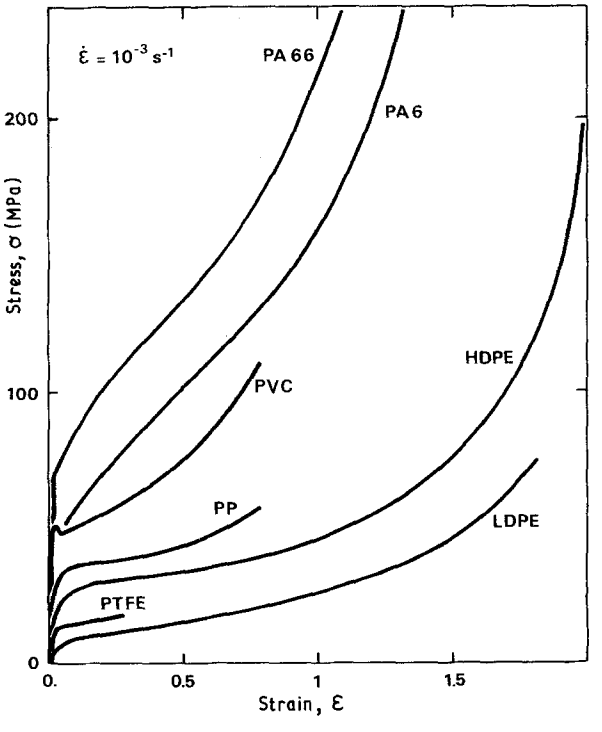

Figure 2 True stress against true strain curves obtained from the data of Fig. 1.

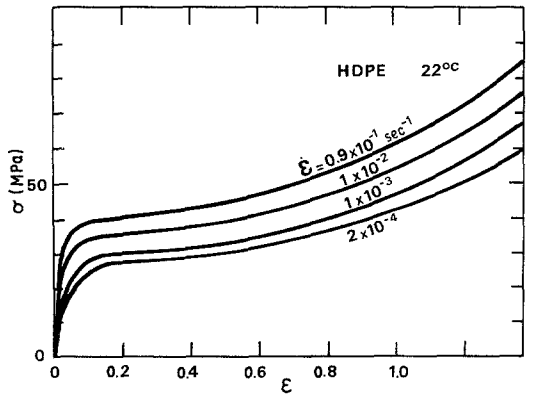

Figure 3 Influence of true strain rate on the stress against strain curves for high density polyethylene at strain rates from 10^{-4} to 10^{-1} sec^{-1}.

3. Yielding and strain rate change behaviour

3.1. Yielding behaviour

Traditionally, the large drop in the tensile force at the beginning of the plastic range has been taken as the principal feature of the mechanical behaviour of ductile polymers. Thus several authors [6–10] have derived constitutive equations on the basis of the nominal stress–strain curves obtained from conventional tests. However, after the pioneer work of Vincent [11], some researchers [12–14] have focussed attention on the geometric origin of the force drop and on the necessity of dealing with true stress–strain curves based on the current diameter of the neck. The data recorded in the present work take this requirement into account. In addition, the constant true strain rate condition reduces the effect of adiabatic heating, which frequently occurs in conventional tests while the neck is forming [15, 16]. Furthermore, due to the slow strain rates used in our tests, the data presented below can be considered to have been determined isothermally.

The shapes of the $\sigma(\epsilon)$ curves in Fig. 2 indicate that, for all the polymers tested except PVC, the drop after the load maximum can be attributed to the decrease in cross-section in the vicinity of the neck. That is, the force drop arises, despite the continuously increasing true stress, because the local decrease in cross-section is greater than the associated increase in flow stress. The curves for low density and high density polyethylene (LDPE and HDPE), for Teflon (PTFE) and for polypropylene (PP) are characterized by a rounded-off yield knee, followed by a plastic stage with a small initial slope and a gradually increasing consolidation rate $d\sigma/d\epsilon$. Neither curve for the polyamides (PA 6 and PA 66) exhibits a yield drop, and these have a slightly different shape: after a sharp knee, the consolidation rate has a large value at first; it then decreases a little and finally increases gradually as for the preceding materials. This is why the tensile force reaches its maximum at a rather large overall strain. The case of polyvinylchloride (PVC) is clearly altogether different since a small (but significant) true stress drop is definitely present. After the stress has stabilized itself at the lower yield point, the rest of the curve is normal, with an increasing slope. It appears therefore that the yield stage is different in the various polymers. Conversely, the plastic range has similar features in all the tested polymers in that the flow stress increases continuously with strain.

The influence of strain rate on the yield behaviour is illustrated in Fig. 4 for the contrasting cases of PVC and HDPE. For this purpose, the flow curves were all normalized to give the same values of stress at $\epsilon = 0.2$ as that obtained at a strain rate of 10^{-3} sec^{-1}. The differences between the curves are thus characteristic of the yield behaviour alone. It can be seen that these differences are not very pronounced. For HDPE, the apparent modulus increases with strain rate and the yield transition is more abrupt. For PVC, the apparent initial modulus is not markedly affected by the strain rate, while the yield transition presents some evolution: the upper yield stress is raised about 5% by a tenfold increase in strain rate and the width of the yield "bump" tends to increase as well.

3.2. Transient behaviour after a stress rate change

The use of strain rate changes to determine rate sensitivity has been widely developed in the case of metals (see for example [17, 18]). It consists of imposing a sudden change in strain rate on the specimen and of recording the resulting change in flow stress. For metals, because of the extended range of homogeneous deformation, a strain rate increase or decrease can be readily effectuated simply through a velocity change of the machine crosshead. Nevertheless, the results must be interpreted carefully because of the influence of the elastic deformation of the testing machine, as well as of the specimen elastic and plastic strains [19, 20].

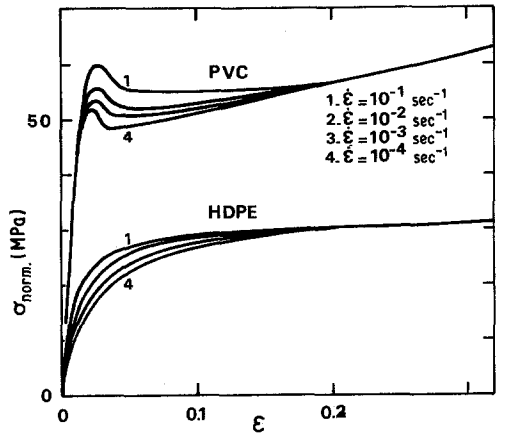

Figure 4 Influence of true strain rate on the yield behaviour of high density polyethylene and polyvinyl chloride. In order to emphasize this effect, the experimental curves are normalized to give the same transient-free level at $\epsilon = 0.2$ as that obtained at 10^{-3} sec^{-1}.

In the case of polymers, strain rate changes have been less widely applied for the derivation of activation analysis data. Such tests have, for example, been performed on PVC by Pink [21], who pointed out the difficulty linked to the early development of a neck in these ductile polymers. If the conventional tensile test is used, the strain rate change can be rigorously applied only at the moment when the load passes through its maximum. Before this point the plastic regime is not yet generalized, and after, a change of elongation rate has complex effects affecting not only the intrinsic material strain rate but also the distribution of strain along the profile of the necked specimen. This problem of the inhomogeneity of the strain was avoided with the new type of test used in the present work. Since the tensile machine controls the local true strain and not the

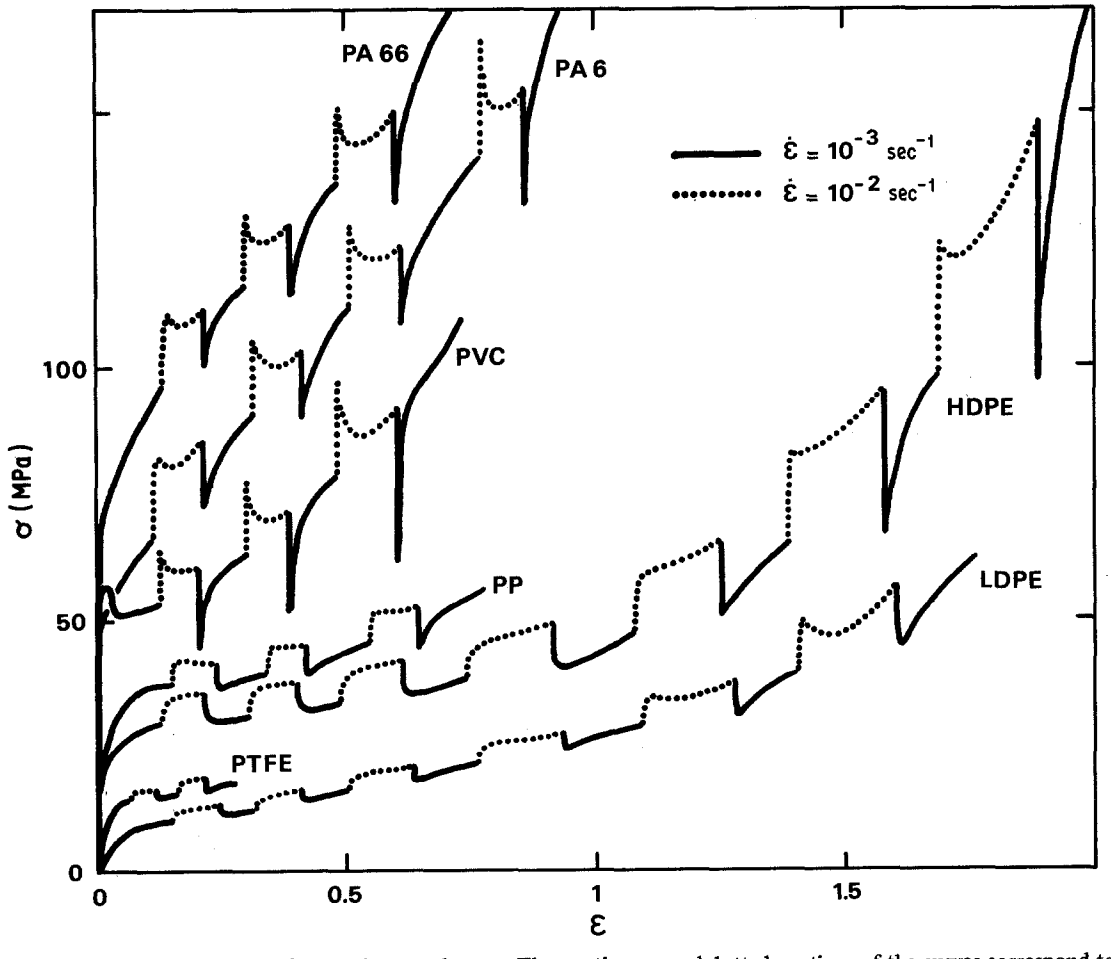

Figure 5 Transients observed after strain rate changes. The continuous and dotted portions of the curves correspond to strain rates of 10^{-3} and 10^{-2} sec^{-1}, respectively.

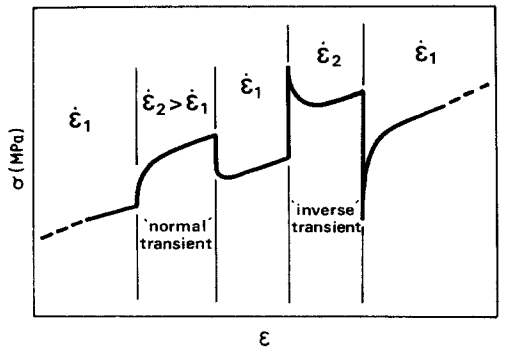

Figure 6 Schematic representation of the idealized "normal" and "inverse" transients produced by strain rate changes.

overall specimen elongation, the strain rate change technique remains valid during the entire test, until rupture. The change is simply produced by a sudden modification in the setting of the function generator which controls the machine.

The curves in Fig. 5 show the results of experiments in which the true strain rate, nominally equal to 10^{-3} sec^{-1}, was changed to 10^{-2} sec^{-1} for selected intervals of time. For all the polymers tested, it can be seen that, after a strain rate change (upward or downward), the tensile flow stress displays a transient curve, the detailed shape of which depends on the material and on the strain. The transient curves persist for strains of about 0.1 to 0.2, after which the stress attains the value it would have reached if the new strain rate had been used from the beginning of the test. The "memory" of the previous strain rate is thus kept conserved only during the transient part, while the behaviour after the transient part seems to be nearly independent of the plastic history and to depend only on the current strain and strain rate.

A closer observation of the curves shows that the transient part can always be considered as intermediate between the two extremes depicted in Fig. 6:

(i) The "normal" transient, characterized by a rounded shape of the stress–strain curve. (Note, however, that when the strain rate is decreased, the stress change is somewhat more abrupt, i.e. sharper than when it is increased.)

(ii) The "inverse" transient, characterized by a marked overshoot of the true stress, before decreasing towards the constant strain rate level. These overshoots have nothing to do with machine inertia effects. They are observed at fast and slow strain rates (even 10^{-4} sec^{-1}), and are due to the intrinsic response of the material. Here again, the downward transient is more abrupt than the upward one.

It should be remarked that, in the case of polyethylene, Teflon and polypropylene, the transients are of the "normal" type when the rate changes are imposed at small strains, while they adopt more and more of an "inverse" character at larger strains. The case of HDPE is eloquent in this respect since the first upward change ($\epsilon = 0.13$) is followed by a very gradual increase in stress, while the last upward change before rupture (initiated at $\epsilon = 1.7$) is followed by a very sharp stress increase with an overshoot larger than 10 MPa.

Conversely, the transients displayed by the PVC and both polyamides are of the "inverse" type even at the first change initiated at $\epsilon \cong 0.13$. The overshoot is particularly marked in the case of PVC. For PA 6 and PA 66, the "inverse" character of the transient is also well marked; however, for the first jump, the stress overshoot is slightly rounded.

4. Transient behaviour after stress relaxation or specimen unloading

4.1. Transient behaviour after stress relaxation

A particularly interesting case of strain rate change is when the new total strain rate is zero, which corresponds to the well-known relaxation test. This has been widely used with polymers (e.g. [22–24]) for the derivation of viscoelastic parameters. However, in our case, we will prefer to focus our attention on the subsequent behaviour of the material, when the test is resumed at the initial strain rate. Such "relax-and-resume" tests have already been studied in detail by Kramer [6] in the course of conventional tensile tests on polyamide specimens. But there again, the early development of a neck permitted the results to be influenced by the change in specimen geometry, so that the microstructural interpretations proposed by the author are open to question.

The curves displayed in Fig. 7 typify the results of tests performed at a constant true strain rate of 10^{-2} sec^{-1}, interrupted several times for periods of 2 min, during which the total strain was held constant. This was accomplished by holding the diameter of the specimen constant. Because the data are presented in the form of σ against ϵ rather than σ against time, this figure does not actually show the relaxation kinetics. Nevertheless, the

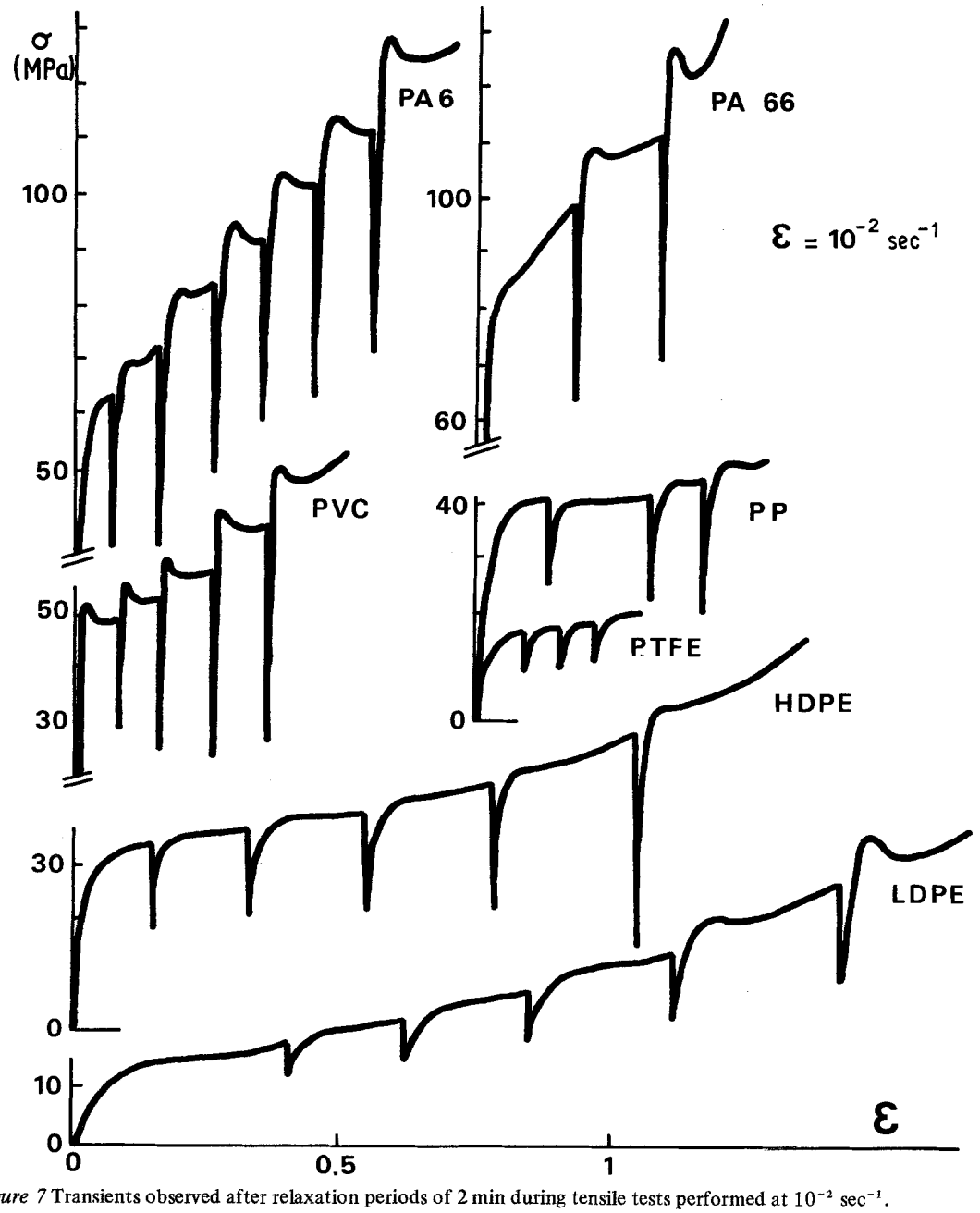

Figure 7 Transients observed after relaxation periods of 2 min during tensile tests performed at 10^{-2} sec^{-1}.

magnitude of each 2 min stress decrease is readily evident, as well as the shape of the true stress–strain curve after straining is resumed at 10^{-2} sec^{-1}. There is considerable similarity between this behaviour and the results of the strain rate changes displayed in Fig. 5. For LDPE, HDPE, PTFE and PP, the σ–ϵ curve rejoins the continuous curve in a gradual and rounded way, except at high strains ($\epsilon > 1$), where a more and more marked overshoot is observed. For PVC, periods of stress relaxation are followed by a sharp overshoot, even at small strains. (It is interesting to note that the overshoot peak observed after the first relaxation period performed at $\epsilon = 0.08$ has exactly the same shape as the true yield peak observed at the beginning of the tensile test.) Finally for PA 6 and PA 66, the relax-and-resume behaviour is similar to that of PVC, except that at strains less than 0.2, no overshoot peak is observed.

The influence of relaxation time was also studied for the typical case of PVC. In Fig. 8, a test is illustrated in which a PVC specimen was subjected

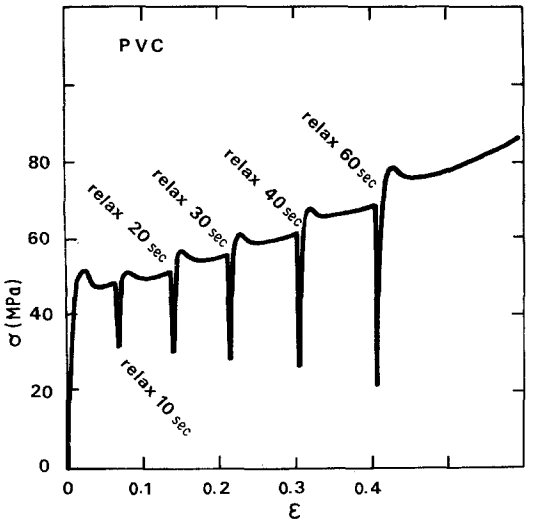

Figure 8 Influence of the duration of stress relaxation in PVC on the height of the subsequent stress peak.

to successive relaxations for times of 10, 20, 30, 40 and 60 sec. The stress dip during the relaxation and the subsequent overshoot peak both increase with the holding time. It appears that this evolution is especially marked for short relaxations, and tends to saturate for holding times longer than 20 sec. In another test, with relaxation continuing for 4.5 h, the overshoot peak following the relaxation has an amplitude comparable with the one developed after a 60 sec relaxation. As in the case of strain rate changes, it was observed that no memory of the relaxation was conserved by the material once the transient period has passed.

4.2. Transient behaviour after unloading

A reduction of stress can be produced during a tensile test by imposing a rapid decrease in the true total strain. This is physically obtained by letting the tensile specimen retract; usually, in the present method, this operation is done through the closed-loop control of the corresponding *increase* in the specimen diameter. The results presented in this section concern experiments in which the unloading operations were arranged so as to reduce the stress to zero.

A typical example is displayed in Fig. 9 for the case of a PVC specimen which experienced three successive unloadings, each lasting 2 min. During these periods, in order to maintain the stress equal to zero, the actuator had to be extended periodically because the specimen tended to contract gradually and thus to generate a tensile stress. It should be remarked that, when the test was resumed after each unloading, the stress gradually rejoined the continuous curve, without any overshoot peak, unlike the curve that follows a relaxation.

Other tests showed that the behaviour exhibited by PVC after unloading is common to all the tested polymers: unloading is always followed by a gradual transient without true stress overshoot peaks.

4.3. Transient behaviour after stress relaxation followed by unloading

Not only does an unloading period produce no overshoot when the test is subsequently resumed, but it can annihilate the effect of a previous relaxation period. Fig. 10 illustrates the shapes of the transients determined on PVC after three composite interruptions consisting of 2 min relaxation periods at constant total strain, followed by an unloading operation which was maintained for 12,

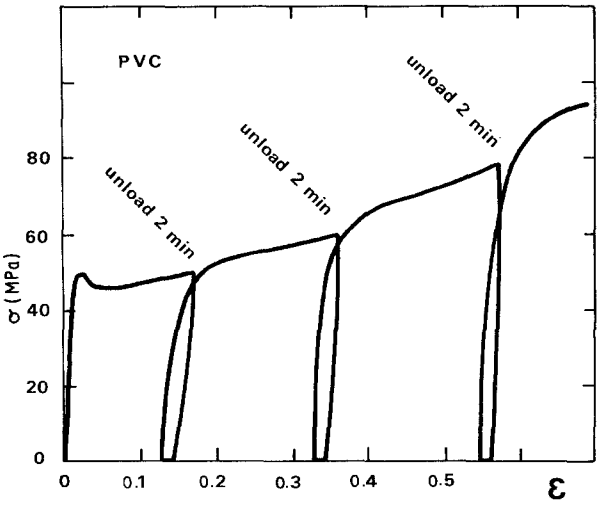

Figure 9 The "normal" transients observed with PVC when the tensile test is resumed after interruptions during which the specimen is unloaded for 2 min.

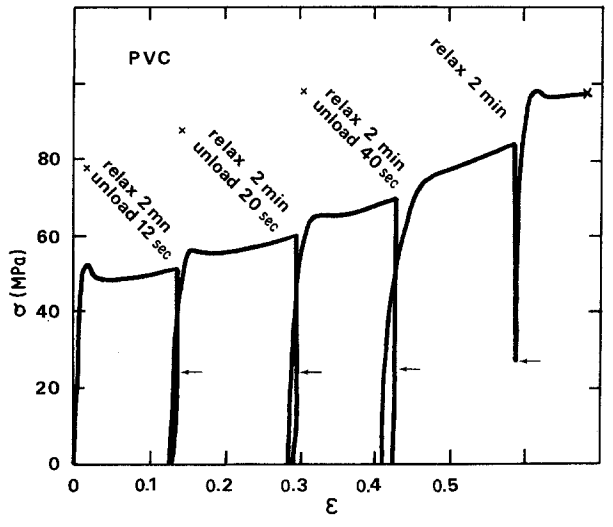

Figure 10 Effect of specimen unloading following periods of stress relaxation in PVC. (The arrows show the minimum stress levels attained during the 2 min relaxations.)

20 or 40 sec. The test was finally completed by imposing a simple relaxation period without further unloading. It is evident from this test that no overshoot period is observed when a relaxation is followed by unloading, provided this latter period is at least 20 sec long. For shorter unloading periods (e.g. 12 sec), the effect of the previous relaxation is only partially erased and a small peak persists when the test is resumed. The normal result of the final relaxation (i.e. the marked peak) shows that none of these observations depends on the previous history of the specimen. Complementary experiments performed with PA 6 and PA 66 specimens revealed effects similar to those depicted in Fig. 10 for the case of PVC.

5. Discussion

5.1. Interpretation of the constant strain rate behaviour of the tested polymers

Before proceeding further in the discussion of the *transient* behaviour of the present polymers, it will be useful to interpret the constant strain rate behaviour on the basis of a simple mechanical model. For this purpose a constitutive equation relating to the stress σ with the strain ϵ and the strain rate $\dot{\epsilon}$ has been selected. The data used for the analysis that follows consisted of about 150 stress–strain curves similar to those of Fig. 2, performed at constant strain rates ranging from 10^{-4} to 10^{-1} sec^{-1}. As noted in the preceding section, under these conditions, the flow stress is an increasing function of both strain ϵ and strain rate $\dot{\epsilon}$. It is evident from these curves that one can derive a large number of mathematical equations $\sigma(\epsilon, \dot{\epsilon})$ all of which adequately fit the entire set of experimental results. However, some of these forms are either more convenient for further use, or more appropriate with regard to microstructural modelling. In a previous paper [1], a preliminary analysis was published which led to a constitutive relation $\sigma(\epsilon, \dot{\epsilon}) = \sigma_1(\epsilon) \times \sigma_2(\dot{\epsilon})$ where the two variables could be separated in the form of two multiplicative functions $\sigma_1(\epsilon)$ and $\sigma_2(\dot{\epsilon})$. This form proved to be particularly convenient for analysing the development of plastic instability in tensile specimens [25, 26] and fitted the experimental data reasonably well over the range of strains and strain rates covered by the usual tensile experiments.

However, most studies of polymer plasticity (see, for example, Pink [21], Andrews and Ward [27], Ward [28] and Bauwens-Crowet *et al.* [29]) have shown that, over a large range of strains and strain rates, the experimental data are better fitted with an additive equation of the type

$$\sigma(\epsilon, \dot{\epsilon}) = \sigma_i(\epsilon) + \sigma^*(\dot{\epsilon}). \quad (1)$$

In such a representation, illustrated schematically in Fig. 11, stress–strain curves at different strain rates are separated by a simple vertical shift. We will now discuss the physical significance of both terms of this equation, and then check the applicability of the equation to our present results. The first term $\sigma_i(\epsilon)$ represents the internal stress and measures the effect of the true plastic strain accumulated in the material during the previous mechanical history of the specimen. As stated by

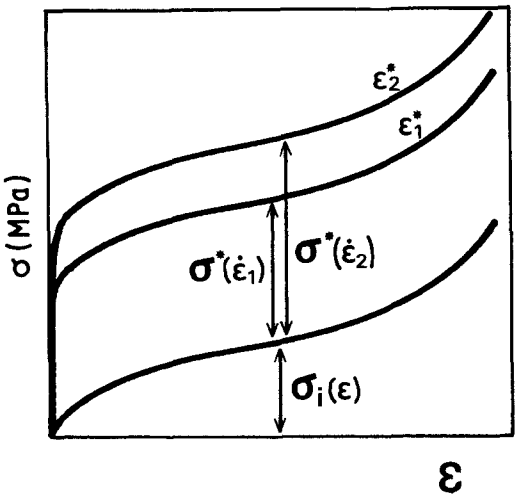

Figure 11 Pictorial representation of the "internal" stress σ_i (which depends on strain) and "effective" stress σ^* (which depends on strain rate).

Fotheringham and Cherry [30, 31], this internal stress acts as a backward driving force which tends to return the material to its undeformed state. It has indeed been shown [32–34], that a plastically deformed polymer can recover its initial shape completely, in tension as well as in shear, provided the thermal or geometrical conditions allow this recovery to be completed within the experimental time.

The exact microstructural origin of the internal stress and its preferred mathematical form are difficult to specify with certainty, especially in the case of semi-crystalline polymers, where the respective contributions of the crystalline lamellae and amorphous layers cannot be understood simply [35, 36]. However, given the common macromolecular nature of all polymers, the internal stress can be considered to be due to the rubberlike entropic forces which make the chains retract when they are unloaded after an elongation. Some of the functions which have been proposed in the literature for this rubberlike elasticity have been reviewed by Treloar [37]. For the sake of simplicity, and considering the relatively small strains experienced by solid ductile polymers in comparison with real rubbers, we have applied the original analysis of Treloar [38] which can be readily adapted to true stress and true strain, and leads to the relation: $\sigma_i(\epsilon) = K[\exp(2\epsilon) - \exp(-\epsilon)]$, where K is a constant. The validity of this equation can be assessed from Fig. 12, where the flow curves of Fig. 2 have been replotted as a function of $[\exp(2\epsilon) - \exp(-\epsilon)]$. It is apparent that the experimental data fit fairly well, except at low strains. (As will be demonstrated below, this discrepancy can be attributed to the effect of the non-negligible values of elastic and viscoelastic strain rate during the initial loading of certain polymers; the associated decrease in plastic strain rate produces the decrease in σ^* at small strains.) The values of the coefficient K were derived from this plot and ranged from 2.2 MPa (LDPE) to 16.8 MPa (PA 66), reflecting the different strain hardening capacities of the present materials. Note that the σ-axis intercepts correspond to the term σ^* of the general equation.

The second term $\sigma^*(\epsilon)$ of the constitutive equation, traditionally called the "effective" stress, reflects the strain rate sensitivity of the material. As frequently explained in the literature [27–29], it can be determined from the σ against $\log(\dot{\epsilon})$ plots displayed in Fig. 13, which are in turn based on constant strain rate data measured at $\epsilon = 0.2$. It can be seen that the experimental points for each polymer are aligned on straight lines within a narrow error band.

This approach, which has been widely used in simple or modified form [10, 29, 39, 40], leads to the relation

$$\dot{\epsilon} = \dot{\epsilon}_0(T) \exp\left(\frac{v_a \sigma^*}{kT}\right) \qquad (2)$$

where k is the Boltzmann constant and v_a, called the "apparant activation volume" is the parameter which characterizes the strain rate sensitivity of the material. The pre-exponential term $\dot{\epsilon}_0(T)$ incorporates both the probability of thermally aided deformation (i.e. the activation energy term) and the dependence of the microstructure on temperature. For the range of strain rates used in the present work, the activation volumes deduced from Fig. 13 range from 1.5 nm^3 (PA 6) to 4.7 nm^3 (PTFE). By combining data from Figs 12 and 13, the pre-exponential factors $\dot{\epsilon}_0$ were found to range from 4×10^{-8} sec^{-1} (LDPE) to 1×10^{-23} sec^{-1} (PA 66) at 22° C.

It is tempting to interpret the above results in terms of a microstructural model in which the plastic strain is achieved by the operation of a single type of elementary process whose volume of influence is equal to the measured activation volume. Although such an approach has been frequently applied to the mechanical behaviour of glassy polymers [41–44], it has recently been

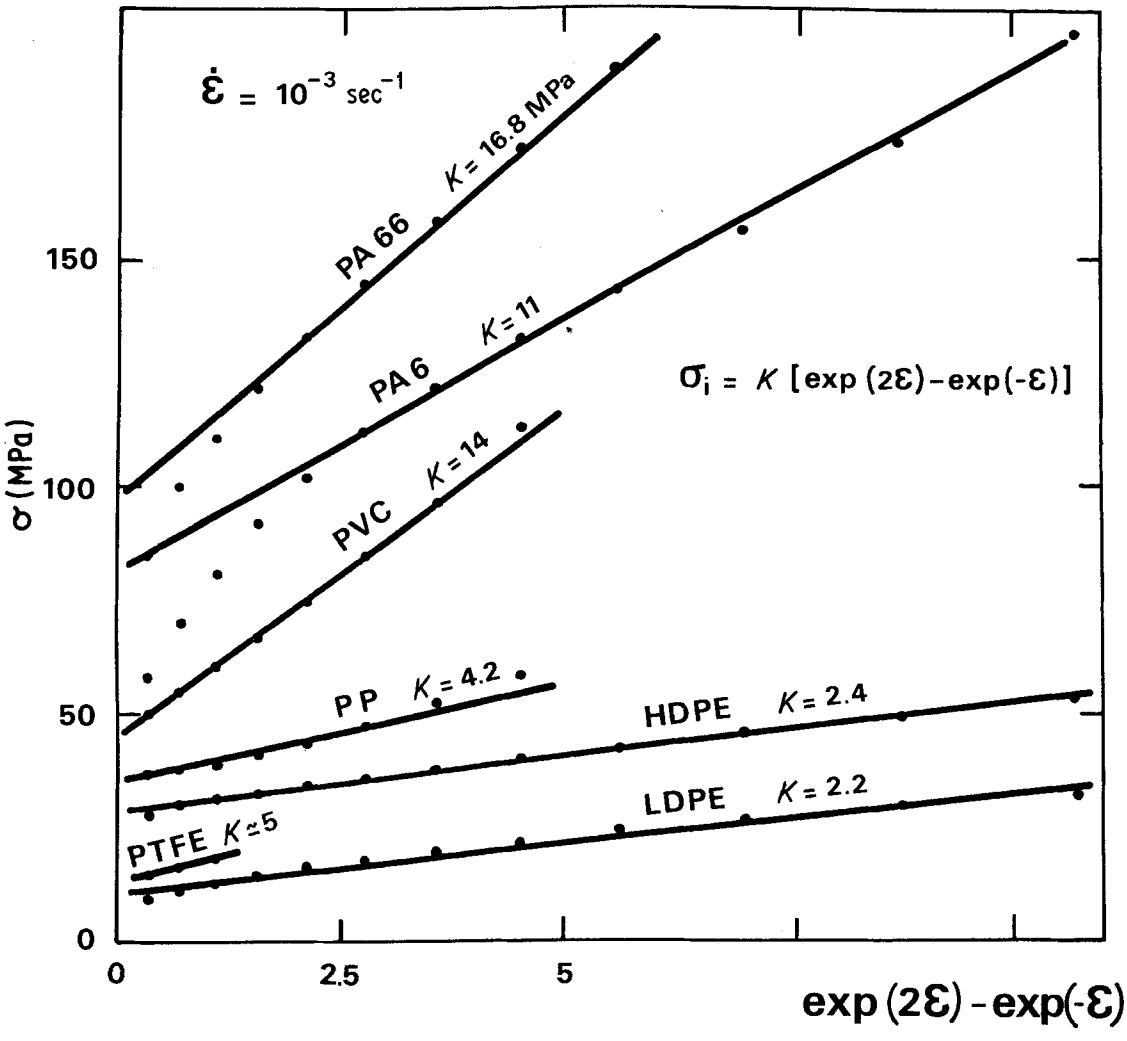

Figure 12 Determination of the coefficient K in the strain hardening equation $\sigma_i(\epsilon) = K[\exp 2\epsilon - \exp(-\epsilon)]$. Dots refer to experimental values; solid lines to the fitted equation.

shown by Escaig [45] that the validity of "single process" activation analysis is limited to very low temperatures, at which no microstructural changes occur, and the activation volume is restricted to a few tenths of a nm^3. (This corresponds to a mechanism which can spread its effects to a limited number of molecular "cages".) Following this author, experimental activation volumes as large as the present ones are taken to signify that changes in microstructure *do* accompany the changes in strain rate and may even completely screen the single mechanism activated process. It will be shown below, however, through the introduction of a simple model, that both the microstructural changes as well as the basic thermally activated mechanism can be revealed by a study of the transient behaviour following rapid changes in strain rate.

5.2. A model for the deformation behaviour of polymers

In the above analysis, the behaviour of the materials was expressed in terms of the total true strain. For a more realistic treatment, it is necessary to decompose the total strain into three components

$$\epsilon = \epsilon_{el} + \epsilon_{visc} + \epsilon_{pl}. \qquad (3)$$

The elastic strain ϵ_{el} due to the deformation of intramolecular bonds, is immediately recoverable and is characterized by a high modulus E, so that it can be expressed to a first approximation as

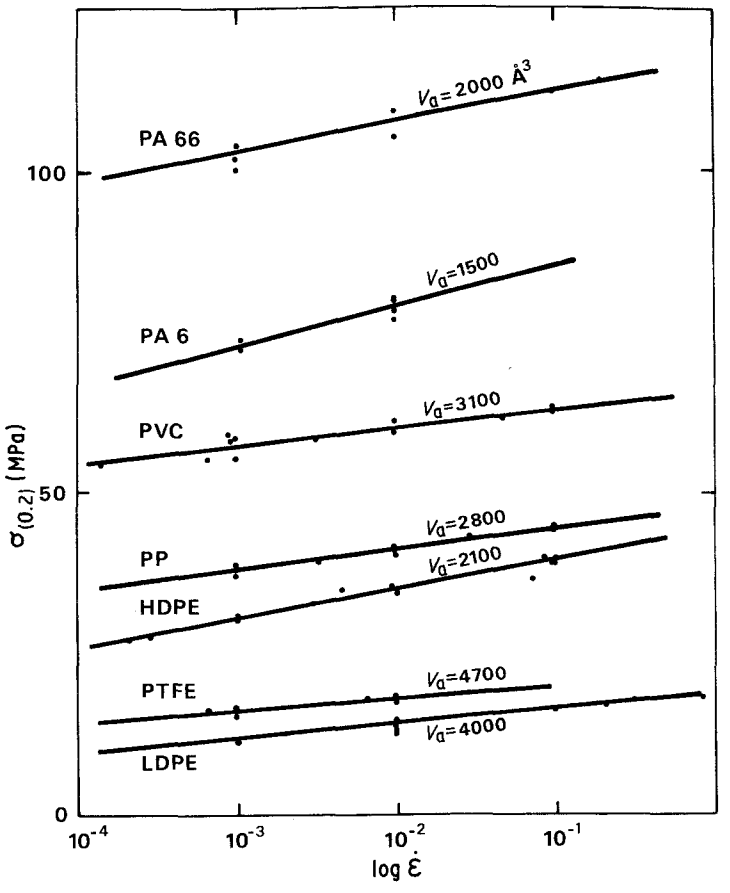

Figure 13 Determination of the parameters v_a and $\dot{\epsilon}_0$ which define the transient-free effective stress $\sigma^*(\dot{\epsilon}) = kT/v_a \cdot \ln(\dot{\epsilon}/\dot{\epsilon}_0)$.

$$\epsilon_{el} = \frac{\sigma}{E}. \quad (4)$$

The viscoelastic strain ϵ_{visc}, associated with the limited retarded movement of amorphous chains, is largely recoverable within a short time scale and is homogeneously distributed within the amorphous parts of the specimen. It is responsible for the generation of an internal or back stress in the regions in which it has taken place. The viscoelastic response can be large only in polymers whose glass transition temperature is lower than the testing temperature. For polyamides and rigid PVC, the amorphous fraction is in a glassy state and so its viscoelastic contribution is small. For polypropylene and polyethylene, the amorphous fraction is rubbery and so it can make a significant viscoelastic contribution to the total strain. The case of Teflon is less clear since general handbooks [46] give its T_g as far above room temperature, but some calorimetric studies [47] have shown that the *real* glass transition of the amorphous fraction is about $-113°$ C. (Our results are consistent with Teflon having a rubbery nature at 22° C.) Although an intensive effort has been made in the past for deriving correct viscoelastic laws, the analyses often remain formal and disconnected from microstructural considerations. The viscoelastic equation obtained from the classical Voigt–Kelvin analogy $\dot{\epsilon}_{visc} = (\sigma/E_v - \epsilon_{visc})/\tau_R$ (where τ_R is the mean retardation time and E_v the relaxed modulus) is a first step toward a phenomenological description of the viscoelastic contribution. It expresses indeed the gradual decrease of the viscoelastic strain rate as this mechanism proceeds in the course of a tensile test. In terms of microstructural evolution one can consider that the viscoelastic capability of the amorphous chains are locally stretched. However it is known that the rheological analogy gives a viscoelastic response which is too sharp: the real behaviour can spread over periods of time which are quite longer than the mean retardation time. Furthermore, when the strain is increasing, the relaxed modulus should be increased gradually.

Lastly, the plastic strain ϵ_{pl} is of a different nature. It has been shown several times [48–51],

in amorphous as well as in semicrystalline polymers, that plastic deformation has a fundamentally inhomogeneous nature. It proceeds by local shearing within deformation bands, which can be narrow or more diffuse according to the material. During this shearing process, the molecules are forced to elongate, so that they experience an increasing shear back stress giving rise to an internal stress σ_i in the plastically deformed regions. The constitutive equation of flow must be applied to the *plastic* component of the strain rate: $\dot{\epsilon}_{pl} = \dot{\epsilon}_0(T) \exp(v_a\sigma^*/kT)$. The previous determination of v_a and $\dot{\epsilon}_0$ remains valid since it was carried out in the post-yield regime, in which the elastic and viscoelastic contributions can be neglected with respect to the plastic strain.

A simple computation based on the above expressions for $\dot{\epsilon}_{el}$, $\dot{\epsilon}_{visc}$ and $\dot{\epsilon}_{pl}$ and on experimental values of the parameters E, E_v, τ_R, $\dot{\epsilon}$, v_a and K, makes it possible to model the constant strain rate $\sigma(\epsilon, \dot{\epsilon})$ curves as well as some aspects of the transient response. Although such an approach leads to a good description of "normal" yielding and "normal" transients, it utterly fails to describe the true yield drop in PVC and the "inverse" transients in general, whatever the values of the experimental parameters. The description of *inverse* transient behaviour requires a modification of the plastic deformation model and one method of doing so will now be described.

As proposed earlier [42–45], plastic shearing in deformation bands cannot proceed by a homogeneous in-phase movement of all the chains bonding the glide plane since this would require a very large stress. Alternatively, it seems more realistic to imagine a model in which localized molecular misfits (or plastic waves) of linear character can be nucleated and then propagate under the influence of the effective stress until they reach the surface or interact with plastic waves travelling on intersecting planes. (Because of the axisymmetric geometry of round specimens, glide occurs on an infinitude of planes and interactions are frequent.) The plastic strain rate can be written by analogy with the Orowan formula, as

$$\dot{\epsilon}_{pl} = \rho(\sigma^*, \epsilon) \cdot v(\sigma^*) \cdot \bar{b}. \tag{5}$$

Here ρ is the length of plastic wave per unit volume, v is the mean velocity of wave propagation and $\bar{b}$ is a mean distance characterizing the elementary shear displacement caused by the passage of a wave.

At a fixed temperature, the wave velocity is controlled by the effective stress and can be expressed as

$$v(\sigma^*) = v_0' \exp\left(-\frac{\Delta G_0^v - w\sigma^*}{kT}\right) = v_0 \exp\left(\frac{w\sigma^*}{kT}\right) \tag{6}$$

where ΔG_0^v is the total activation free enthalpy and w is the activation volume of the propagation process. The total length of plastic wave during transient-free deformation $\rho_{t.f.}$, which characterizes the deformation microstructure, also depends on the effective stress, and can be written as

$$\rho(\sigma^*)_{t.f.} = \rho_0' \exp\left(-\frac{\Delta G_0^r - r\sigma^*}{kT}\right) = \rho_0 \exp\left(\frac{r\sigma^*}{kT}\right) \tag{7}$$

where ΔG_0^r is the total activation free enthalpy and r is the activation volume for wave nucleation.* Under these conditions, the strain rate given by the model

$$\dot{\epsilon}_{pl} = \rho_0' v_0' \bar{b} \exp\left(-\frac{\Delta G_0^r + \Delta G_0^v}{kT}\right) \exp\left[\frac{(r+w)\sigma^*}{kT}\right] = \rho_0 v_0 \bar{b} \exp\left[\frac{(r+w)\sigma^*}{kT}\right] \tag{8}$$

is at least in formal agreement with the experimental relation

$$\dot{\epsilon}_{pl} = \dot{\epsilon}_0 \cdot \exp\left(\frac{v_a\sigma^*}{kT}\right) \tag{9}$$

with $v_a = r + w$ and with the overall activation free enthalpy $\Delta G_0 = \Delta G_0^r + \Delta G_0^v$.

The model described above is not yet able to explain the experimentally observed "inverse" transients. For this purpose, we will adopt the approach of Gilman and Johnston [52] and assume that, although the wave velocity can change instantaneously with σ^*, the wave density can only increase *gradually* as straining proceeds, since a given wave must expand from its nucleus in order to increase its length. In the original

*Note that nucleation and propagation need not both be thermally activated. It is their *stress dependence* which is of particular interest here. If one or other is entirely mechanically activated, the "activation volume" simply loses its physical significance and becomes a coefficient of stress dependence.

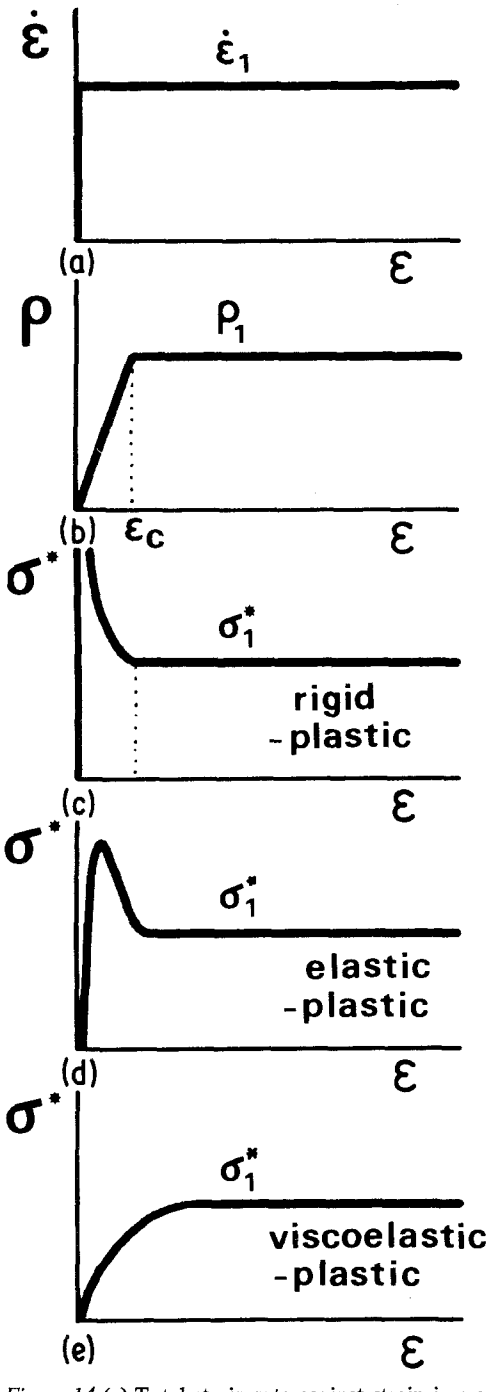

Figure 14 (a) Total strain rate against strain in a constant strain rate test, (b) the linear strain dependence of the plastic wave density called for by the present model. Evolution of the effective stress against strain for: (c) a rigid–plastic polymer, (d) an elastic–plastic polymer and (e) a viscoelastic–plastic polymer.

Gilman–Johnston model, the wave density was a monotonically increasing function of strain. We propose alternatively that, whenever a polymer experiences a strain rate increase or decrease, the plastic wave density changes accordingly over a particular strain interval ϵ_c until it reaches the new equilibrium value characteristic of the new strain rate. This approach is in agreement with the earlier suggestion of Brown and Ward [53], that, for some glassy polymers, the intrinsic yield drop is due to the difference between the conditions for the *initiation* of yielding and for the *propagation* of transient-free flow.

5.3. Interpretation of the transients

5.3.1. Yield behaviour

The yielding of polymers is a particular case of a strain rate change from an initial value $\dot{\epsilon}_i = 0$ to a final $\dot{\epsilon}_f = \dot{\epsilon}_1$. If it is first assumed that the material has an ideal rigid-plastic behaviour (elastic modulus $E = \infty$, viscoelastic time $\tau_v = \infty$), then the rate change must be immediately accommodated by the plastic strain rate $\dot{\epsilon}_{pl}$ which jumps from 0 to $\dot{\epsilon}_1$ (Fig. 14). As a first approximation, the increase in wave density proposed above can be taken to be linear, so that

$$\rho(\epsilon) = \begin{cases} 0 & \text{for } \epsilon = 0 \\ \rho_1 \cdot \dfrac{\epsilon}{\epsilon_c} & \text{for } 0 < \epsilon < \epsilon_c \\ \rho_1 & \text{for } \epsilon > \epsilon_c \end{cases} \quad (10)$$

where $\rho_1 = \rho_0 \exp(r\sigma_1^*/kT)$ is the transient-free value of ρ and $\sigma^* = \sigma_1^*$ after the critical transient interval ϵ_c. This oversimplified linear kinetics does not pretend to represent the real one with accuracy since ρ is certainly a complex function of ϵ and t, but it can nevertheless be used to check whether the main features of the yield response can be grossly interpreted on this basis. We can then write

$$\dot{\epsilon}_{pl} = \dot{\epsilon}_1 = \left(\rho_1(\sigma_1^*) \cdot \frac{\epsilon}{\epsilon_c}\right) \cdot v(\sigma^*) \cdot \bar{b}$$

$$= \rho_0 \exp\left(\frac{r\sigma_1^*}{kT}\right) \cdot \frac{\epsilon}{\epsilon_c} \cdot v_0 \exp\left(\frac{w\sigma^*}{kT}\right) \cdot \bar{b} \quad (11)$$

and, since $\rho_0 v_0 b = \dot{\epsilon}_0$ and $r = v_a - w$

$$\dot{\epsilon}_1 = \dot{\epsilon}_0 \exp\left(\frac{v_a\sigma_1^*}{kT}\right) \cdot \exp\left(\frac{w(\sigma^* - \sigma_1^*)}{kT}\right) \cdot \frac{\epsilon}{\epsilon_c}$$

$$= \dot{\epsilon}_1 \exp\left(\frac{w(\sigma^* - \sigma_1^*)}{kT}\right) \cdot \frac{\epsilon}{\epsilon_c} \quad (12)$$

so that

$$\sigma^* = \sigma_1^* + \left(\frac{v_a}{w}\right)\frac{kT}{v_a} \ln\left(\frac{\epsilon_c}{\epsilon}\right) \qquad \text{for } 0 < \epsilon < \epsilon_c \quad (13)$$

and

$$\sigma^* = \sigma_1^* \qquad \text{for } \epsilon > \epsilon_c. \tag{14}$$

The stress–strain curve obtained from this function (Fig. 14c) does indeed exhibit a yield drop whose shape can be adjusted by a suitable choice of the parameters v_a/w and ϵ_c. In particular, it can be seen that the width of the yield drop peak is large if v_a/w is large, that is, if the nucleation mechanical work or activation volume is large compared with the propagation activation volume.

In order to eliminate the unrealistic singularity of the stress at $\epsilon = 0$, the elastic–plastic model will now be introduced. First the total strain rate is held

$$\dot{\epsilon} = \dot{\epsilon}_{el} + \dot{\epsilon}_{pl} = \dot{\epsilon}_1 \tag{15}$$

with

$$\dot{\epsilon}_{el} = \dot{\sigma}/E = \frac{1}{E}\frac{d\sigma}{d\epsilon_T}\frac{d\epsilon}{dt} = \frac{\dot{\epsilon}_1}{E}\frac{d\sigma}{d\epsilon} \tag{16}$$

and

$$\dot{\epsilon}_{pl} = \dot{\epsilon}_1 \exp\left[\frac{w(\sigma^* - \sigma_1^*)}{kT}\right] \cdot \frac{\epsilon}{\epsilon_c}. \tag{17}$$

Under these conditions,

$$\frac{d\sigma}{d\epsilon} = E\left\{1 - \exp\left[\frac{w(\sigma - \sigma_i(\epsilon) - \sigma_1^*)}{kT}\right] \cdot \frac{\epsilon}{\epsilon_c}\right\}. \tag{18}$$

This differential equation cannot be solved analytically, but its numerical integration is straightforward and leads to a stress–strain curve like the one in Fig. 14d. This curve can be taken to describe the experimental yield behaviour of PVC, as the following values were chosen for the experimental parameters: $E = 3300$ MPa, $v_a/w = 8$ and $\epsilon_c = 0.05$. It is thus apparent that the small and abrupt true stress peak which characterizes the basic yield behaviour of glassy polymers can be attributed to the supplement of stress necessary to overactivate the existing plastic waves while a sufficient number of new ones can be nucleated. Such a yield drop has also been observed in polycarbonate [50] and in polyethylene terephthalate [12] by using in both cases a shear testing technique where no geometric effects intervene. The reason why no yield drops appear in the cases of polyethylene, polypropylene and Teflon is that the yield response is rounded off due to their smaller elastic moduli and their larger viscoelastic compliances. Indeed, if the viscoelastic strain rate $\dot{\epsilon}_{visc}$ is introduced into the above analysis, the stress drop can be suppressed completely since the viscoelastic contribution can accommodate a part of the total strain rate at the critical moment when the density of plastic waves has to increase. Finally, in the case of the polyamides, the gradual yielding of the specimens may appear surprising since the glass transition temperatures of the amorphous fractions are above room temperature. However, the observed behaviour can be ascribed to the effect of moisture and added plasticizers, which make possible the movement of viscoelastic chains in these otherwise glassy polymers.

5.3.2. *Transients associated with strain rate changes*

When a polymer currently tested at a strain rate $\dot{\epsilon}_1$ experiences an increase to a higher rate $\dot{\epsilon}_2$, the plastic wave density must adjust itself from the current value ρ_1 to the new value ρ_2 (Fig. 15). Here again, it is assumed that this change of density cannot be immediate and follows a law of the type

$$\rho = \rho_1 \qquad \text{for } \epsilon < \epsilon_j \tag{19}$$

$$\rho = \rho_1 + (\rho_2 - \rho_1)\frac{\epsilon - \epsilon_j}{\epsilon_c - \epsilon_j} \qquad \text{for } \epsilon_j < \epsilon < \epsilon_j + \epsilon_c \tag{20}$$

$$\rho = \rho_2 \qquad \text{for } \epsilon > \epsilon_j + \epsilon_c. \tag{21}$$

Here ϵ_j is the strain at which the increase is initiated and ϵ_c is once again the characteristic strain required to attain the new density ρ_2. For a polymer with an ideal rigid-plastic response, we can follow the method outlined above to obtain

$$\dot{\epsilon}_{pl} = \dot{\epsilon}_2 = \left[\rho_1 + (\rho_2 - \rho_1)\left(\frac{\epsilon - \epsilon_j}{\epsilon_c - \epsilon_j}\right)\right] \cdot v(\sigma^*)\bar{b} \tag{22}$$

$$v(\sigma_2^*) = \left[\frac{\rho_1}{\rho_2} + \left(1 - \frac{\rho_1}{\rho_2}\right)\left(\frac{\epsilon - \epsilon_j}{\epsilon_c - \epsilon_j}\right)\right] \cdot v(\sigma^*) \tag{23}$$

with

$$\frac{\rho_1}{\rho_2} = \exp\left[-\frac{r(\sigma_2^* - \sigma_1^*)}{kT}\right] \tag{24}$$

one gets, for $\epsilon_j < \epsilon < \epsilon_j + \epsilon_c$

$$\sigma^* = \sigma_2^* - \left(\frac{v_a}{w}\right)\left(\frac{kT}{v_a}\right)\ln\left\{\exp\left(-\frac{r\Delta\sigma}{kT}\right) + \left[1 - \exp\left(-\frac{r\Delta\sigma}{kT}\right)\right]\left(\frac{\epsilon - \epsilon_j}{\epsilon_c - \epsilon_j}\right)\right\} \tag{25}$$

where

$$\Delta\sigma = \sigma_2^* - \sigma_1^*. \tag{26}$$

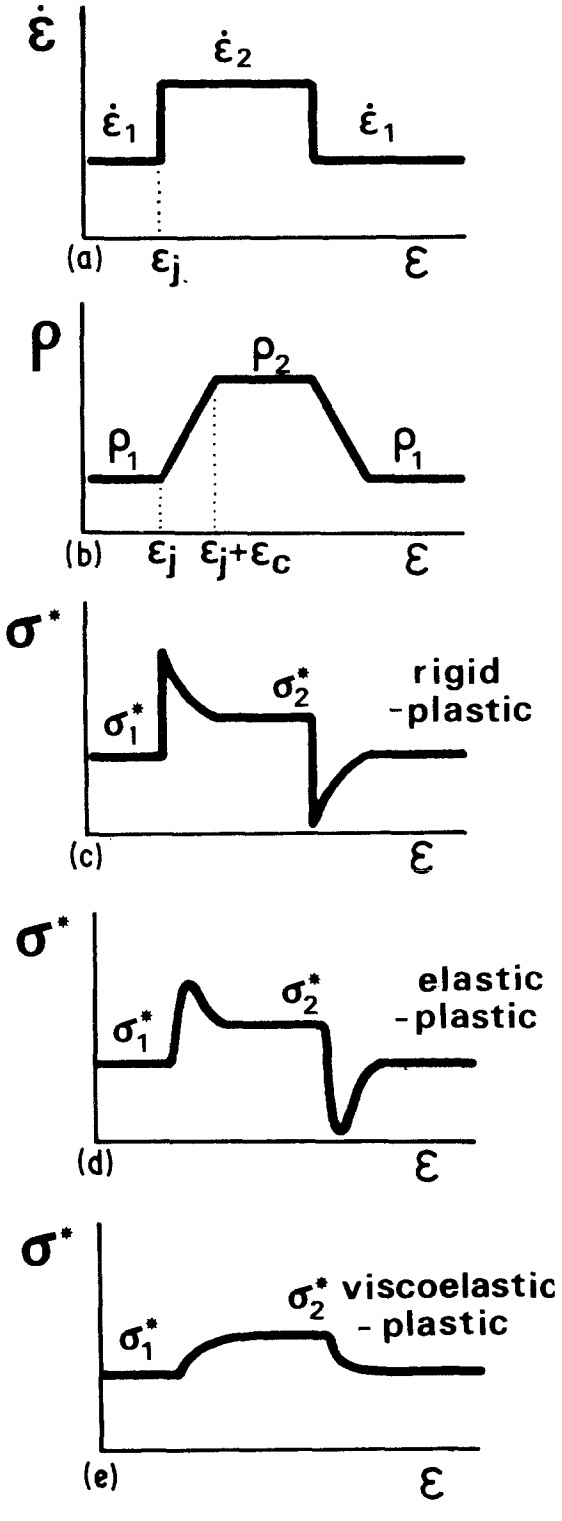

Figure 15 (a) Total strain rate against strain during rapid strain rate changes, (b) the evolution of the wave density prescribed by the current treatment. Evolution of the effective stress against strain for: (c) a rigid–plastic polymer, (d) an elastic–plastic polymer and (e) a viscoelastic–plastic polymer.

The transient behaviour described by this equation is characterized, as indicated in Fig. 15c, by a finite stress overshoot whose amplitude is equal to

$$\sigma^*_{\max} - \sigma^*_2 = \left(\frac{v_a}{w} - 1\right) \Delta\sigma. \tag{27}$$

In the case of a strain rate decrease ($\dot{\varepsilon}_2 < \dot{\varepsilon}_1$), the same equation holds with $\Delta\sigma < 0$, giving rise to the finite stress dip illustrated in Fig. 15c. If the material exhibits elastic–plastic behaviour (Fig. 15d), the numerical procedure introduced above for yielding shows that the upward overshoot is rounded off and decreased. As reported previously for metallic materials [19, 20], the downward stress dip is made deeper by the elastic contribution, which thus explains the generally observed asymmetry of the up-and-down strain rate changes.

Finally, by introducing the viscoelastic contribution, the overshoots and stress dips can be eliminated completely (Fig. 15e). This procedure explains why the transients associated with strain rate changes in a viscoelastic material become sharper and sharper as the current strain is increased. It is the gradual exhaustion of the viscoelastic capability with increasing strain that appears to be responsible for the transformation of the transients from "normal" to "inverse".

5.3.3. Transients after a period of stress relaxation

When the total strain rate is suddenly reduced to $\dot{\varepsilon}_T = 0$, plastic straining continues to proceed and the elastic strain is gradually relaxed. In terms of the present model, the total length ρ of plastic wave in the material also decreases during relaxation, tending towards zero as the stress tends towards the internal stress σ_i (Fig. 16). The quantitative application of this model to the case of an elastic–plastic polymer leads to logarithmic kinetics for the relaxing stress

$$\sigma^* = \sigma^*_0 - \frac{kT}{v_a} \ln\left(\frac{v_a}{kT} \dot{\varepsilon}_1 E t + 1\right) \tag{28}$$

where σ^*_0 is the effective stress at the beginning of the relaxation. This expression, which is similar to the one derived by Guiu and Pratt [54], holds only as long as σ^* is not too close to zero. (In the latter event, the strain rate must be expressed in terms of a hyperbolic sine instead of an exponential, as in the Eyring [55] activation analysis.) From the above expression for σ^*, we can derive the length of residual plastic wave $\rho(t)$ at any moment of the

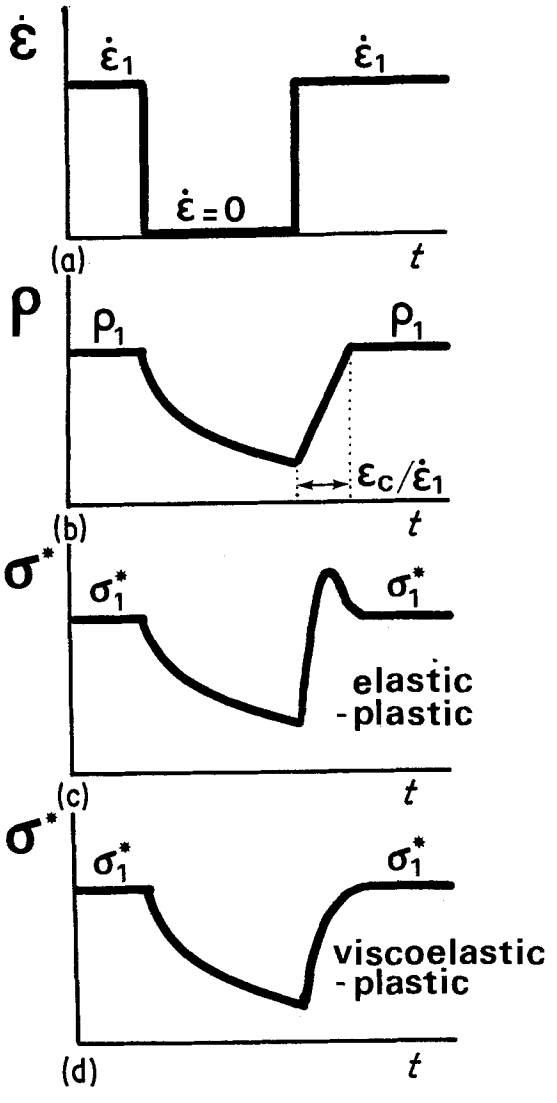

Figure 16 (a) Total strain rate against time in a "deform-relax-resume" test, (b) the wave density is gradually exhausted during the relaxation period. Evolution of the effective stress against time for: (c) an elastic–plastic polymer and (d) a viscoelastic–plastic polymer.

relaxation. If the relaxation is continued for an infinite time, the effective stress is reduced asymptotically to zero, as is the wave density.

When the tensile test is resumed in the course of a relaxation, the situation resembles the case of initial yielding, since the plastic straining must be reinitiated from a microstructural state that contains few plastic waves. (The longer the relaxation, the fewer the remaining plastic waves.) The shape of the flow curve after the test is resumed is then characterized by a stress overshoot. Furthermore, if the "relax-and-resume" test is performed after a high prestrain, the overshoot can no longer be erased by viscoelastic effects, since the viscoelastic strain capability of the material is now nearly exhausted (see above).

5.3.4. Transients after an unloading

When the total stress is set abruptly to zero during a tensile test (i.e. when straining is interrupted and the material is unloaded), the subsequent effects differ radically from those observed after relaxation. In this case, the elastic strain is immediately set to zero, the viscoelastic strain returns to zero more gradually according to its own kinetics (characterized by the retardation time τ_R), and finally, a compressive plastic strain rate appears since the effective stress is reversed in sign when it is set to the negative of the internal stress ($\sigma^* = -\sigma_i$). It appears from the experimental results on PVC that, when the load is removed, the plastic wave population continues to exist even if its mean velocity drops to zero, or to a low value. It does not tend to be exhausted by forward gliding as in the case of stress relaxation. Instead, the small negative strain rate, which is responsible for the anelastic effect observed in Fig. 9, is accompanied by the slow backward glide of some of the waves, as well as by the possible nucleation of new negative shear waves, such that the total density decreases very slowly to the level appropriate to the internal stress.

If the tensile test is resumed after an unloading period (see Fig. 9) no overshoot is observed since the population of available plastic waves is high enough to supply the plastic part of the strain rate while the viscoelastic component is fully depleted. When the sample is relaxed for a long time (exhausting its plastic wave population), prior to unloading for a specific period, and then tensile tested a second time, once again no stress overshoot occurs. Here it can be hypothesized that the negative plastic strain rate established during the unloaded period gave rise to a new set of waves numerous enough to accomodate further tensile testing without a reloading transient. Such reversible glide effects seem to be particularly common in polymers: in a study devoted to the torsion testing of polycarbonate, Wu and Turner [56] showed that the reverse shearing of a pre-deformed polymer could be achieved at a lower stress than the continued forward shearing. This was explained by invoking a kind of Bauchinger effect.

6. Summary and conclusions

The plastic behaviour of seven commercial polymers (low density and high density polyethylene, polytetrafluoroethylene, polypropylene, polyvinyl chloride, polyamide 6 and 66) was investigated at room temperature. The experiments were carried out at constant local true strain rate with the aid of a closed-loop hydraulic tensile machine equipped with an exponential function generator and a diametral transducer. Transients tests were also performed involving: (i) rapid changes in strain rate, (ii) stress relaxation at constant total strain, followed by the resumption of straining and (iii) abrupt loading of the samples for various intervals followed by the resumption of straining. The results obtained permitted the following conclusions to be drawn.

(1) The flow stresses σ determined at constant strain rates $\dot{\epsilon}$ in the range 10^{-4} to 10^{-1} sec^{-1} can be represented by additive constitutive relations of the form $\sigma = \sigma_i(\epsilon) + \sigma^*(\dot{\epsilon})$. Here the effective stress σ^* increases with $\log \dot{\epsilon}$, as given by: $\sigma^* = kT/v_a \cdot \ln(\dot{\epsilon}/\dot{\epsilon}_0)$, where v_a is an experimental activation volume (for the present materials, values in the range 1.5 nm^3 (PA 6) to 4.7 nm^3 (PTFE) were observed) and $\dot{\epsilon}_0$ is an experimental parameter [in the range 10^{-23} sec^{-1} (PA 66) to 4×10^{-8} sec^{-1} (LDPE)]. The internal stress σ_i obeys a relation of the type proposed by Treloar, namely: $\sigma_i = K[\exp 2\epsilon - \exp(-\epsilon)]$; here K is in the range 2.2 MPa (LDPE) to 16.8 MPa (PA 66) and characterizes the rubberlike entropy forces acting on the extended macromolecular chains.

(2) A model in which plastic deformation proceeds by the nucleation and propagation of plastic shear waves describes adequately the constant strain rate, as well as the transient behaviour of the present materials. According to this model, both the nucleation and propagation processes are thermally activated, but with higher apparent activation volumes for the former than for the latter process. In the course of transient-free deformation, the density of plastic waves and their velocity depend only on the effective stress, and thus, like it, remain constant. During transients, the wave velocity changes instantaneously with effective stress; by contrast, the wave density changes more slowly, following the original approach by Gilman and Johnston.

(3) The precise shape of the flow curve at yielding can be determined by the present technique since it is free of geometric and localized self-heating effects. Thus, *true* yield drops are observed in a rigid glassy polymer such as PVC. Conversely, the yield transient is gradual in the rubberlike or plasticized materials. In the latter ones, the elastic and viscoelastic components of strain rate accommodate a large part of the total strain rate during the strain interval necessary for nucleating the plastic waves.

(4) When the strain rate is abruptly increased or decreased, "inverse" transients (characterized by stress overshoots or sharp stress dips) are observed in the polymers with a glassy phase (PA and PVC). By comparison, in those with a rubbery phase (PP, PTFE, HDPE, LDPE), the transients are "normal" at low strains (with gradual changes in stress) and convert to "inverse" at high strains. According to the model, "inverse" transients are observed when the elastic and viscoelastic strain rate contributions are small. "Normal" transients are only obtained at small strains because the required viscoelastic strain contributions is exhausted at high total strains.

(5) When straining is interrupted to permit stress relaxation and then later resumed, a stress overshoot is observed under the conditions which lead to "inverse" transients in (4) above. Conversely, if the load is abruptly removed, a "normal" transient is observed when straining is resumed. According to the model, the difference between these two types of behaviour is attributed, in the first case, to the gradual exhaustion of the plastic waves during the relaxation as the effective stress goes to zero; in the second case, to the maintenance of an appreciable plastic wave density appropriate to the non-zero value of the effective stress ($\sigma^* = -\sigma_i$).

Acknowledgements

The authors are indebted to the Natural Science and Engineering Research Council of Canada and the Ministry of Education of Quebec for financial support. The experimental part of this work was carried out at McGill University during a period of sabbatical leave of one of the authors (CG). For this, he is grateful to the Institut National Polytechnique de Lorraine, as well as for the France–Quebec Research Fellowship awarded by the Ministry of Intergovernmental Affairs of Quebec. The authors also thank Plastifab Industries Inc. of Montreal, Quebec, for kindly supplying the experimental materials.

References

1. C. G'SELL and J. J. JONAS, *J. Mater. Sci.* **14** (1979) 583.
2. P. W. BRIDGMAN, *Trans. Amer. Soc. Met.* **32** (1944) 553.
3. R. HILL, "Mathematical Theory of Plasticity" (Oxford University Press, Oxford, 1950) p. 272.
4. P. F. THOMASON, *Int. J. Mech. Sci.* **11** (1969) 481.
5. A. NEEDLEMAN, *J. Mech. Phys. Sol.* **20** (1972) 111.
6. E. J. KRAMER, *J. Appl. Phys.* **41** (1970) 4327.
7. J. M. ANDREWS and I. M. WARD, *J. Mater. Sci.* **5** (1970) 411.
8. S. BAHADUR, *Polymer Eng. Sci.* **13** (1973) 266.
9. A. CROSS and R. N. HAWARD, *J. Polymer Sci.* **11** (1973) 2423.
10. R. N. HAWARD and G. THACKRAY, *Proc. Roy. Soc.* **A302** (1968) 453.
11. P. I. VINCENT, *Polymer* **1** (1960) 7.
12. N. BROWN and I. M. WARD, *J. Polymer Sci. A-2* **6** (1968) 607.
13. G. MEINEL and A. PETERLIN, *ibid.* **9** (1971) 67.
14. N. J. MILLS, *Brit. Polymer J.* **10** (1978) 1.
15. I. H. HALL, *J. Appl. Polymer Sci.* **12** (1968) 731.
16. A. S. KORHONEN and H. J. KLEEMOLA, *Met. Trans. A* **9A** (1978) 979.
17. H. CONRAD, *Acta Met.* **6** (1968) 339.
18. J. P. IMMARIGEON and J. J. JONAS, *ibid.* **19** (1971) 1053.
19. U. F. KOCKS, A. S. ARGON and M. F. ASHBY, *Prog. Mater. Sci.* **19** (1975) 257.
20. Z. S. BASINSKI, P. J. JACKSON and M. S. DUESBERY, *Phil. Mag.* **36** (1977) 255.
21. E. PINK, *Mater. Sci. Eng.* **23** (1976) 275.
22. L. E. NIELSEN, "Mechanical Properties of Polymers" (Reinhold Publ. Co., New York, 1962).
23. J. D. FERRY, "Viscoelastic Properties of Polymers" (J. Wiley, New York, 1961) pp. 9, 41, 63.
24. J. R. McLOUGHLIN and A. V. TOBOLSKY, *J. Colloid. Sci.* **7** (1952) 555.
25. J. J. JONAS, R. A. HOLT and C. E. COLEMAN, *Acta Met.* **24** (1976) 911.
26. A. K. GHOSH, *ibid.* **25** (1977) 1413.
27. J. M. ANDREWS and I. M. WARD, *J. Mater. Sci.* **5** (1970) 411.
28. I. M. WARD, *ibid.* **6** (1971) 1397.
29. C. BAUWENS-CROWET, J. M. OTS and J. C. BAUWENS, *ibid.* **9** (1974) 1197.
30. D. G. FOTHERINGHAM and B. W. CHERRY, *ibid.* **13** (1978) 231.
31. *Idem, ibid.* **13** (1978) 951.
32. I. L. HAY and A. KELLER, *Kolloid Z. und Z. Polymere* **204** (1965) 43.
33. R. HOSEMAN, J. LOBODA-ČAČKOVIČ and H. ČAČKOVIČ, *J. Mater. Sci.* **7** (1972) 963.
34. J. C. M. LI, *Metall. Trans.* **9A** (1978) 1353.
35. J. L. KARDOS and J. RAISONI, *Polymer Eng. Sci.* **15** (1975) 183.
36. V. PETRACCONE, I. C. SANCHEZ and R. S. STEIN, *Polymer Sci., Phys. Ed.* **13** (1975) 1991.
37. L. R. G. TRELOAR, *Rep. Prog. Phys.* **36** (1973) 755.
38. *Idem, Trans. Faraday Soc.* **39** (1943) 36.
39. C. BAUWENS-CROWET, *J. Mater. Sci.* **8** (1973) 968.
40. S. H. JOSEPH, *J. Polymer Sci.* **16** (1978) 1971.
41. A. S. ARGON, *Phil. Mag.* **28** (1973) 839.
42. P. B. BOWDEN and S. RAHA, *ibid.* **29** (1975) 149.
43. E. PINK, *Rev. Deform. Behav. Mater.* **2** (1977) 37.
44. B. ESCAIG and J. M. LEFEBVRE, *Rev. Phys. Appl.* **13** (1978) 285.
45. B. ESCAIG, *Ann. Phys.* **3** (1978) 207.
46. J. A. BRYDSON, in "Polymer Science" edited by A. D. Jenkins (North Holland, Amsterdam, 1972) pp. 194–249.
47. G. T. FURUKAWA, R. E. McCOSKEY and G. J. KING, *J. Res. Nat. Bur. Stand.* **49** (1952) 273.
48. J. B. C. WU and J. C. M. LI, *J. Mater. Sci.* **11** (1976) 434.
49. P. B. BOWDEN and S. RAHA, *Phil. Mag.* **22** (1970) 463.
50. R. E. ROBERTSON, *J. Polymer Sci. A2* **7** (1969) 1315.
51. P. B. BOWDEN and R. J. YOUNG, *J. Mater. Sci.* **9** (1974) 2034.
52. W. G. JOHNSTON, *J. Appl. Phys.* **33** (1962) 2716.
53. N. BROWN and I. M. WARD, *J. Polymer Sci. A2* **6** (1968) 607.
54. F. GUIU and P. L. PRATT, *Phys. Stat. Sol.* **6** (1964) 111.
55. H. EYRING, *J. Chem. Phys.* **4** (1936) 283.
56. W. WU and A. P. L. TURNER, *J. Polymer Sci.* **11** (1973) 2199.

Received 15 October 1980 and accepted 12 January 1981.